ELSEVIER

Journal of Biomechanics 31 (1998) 535–544

JOURNAL OF BIOMECHANICS

Degeneration affects the anisotropic and nonlinear behaviors of human anulus fibrosus in compression

James C. Iatridis[a,*], Lori A. Setton[b], Robert J. Foster[c], Bernard A. Rawlins[d], Mark Weidenbaum[c], Van C. Mow[c]

[a]*McClure Musculoskeletal Research Center, Department of Orthopaedics and Rehabilitation, University of Vermont, Burlington, VT, U.S.A.*
[b]*Departments of Biomedical Engineering and Surgery, Duke University, Durham, NC, U.S.A.*
[c]*Departments of Mechanical Engineering and Orthopaedic Surgery, Columbia University, New York, NY, U.S.A.*
[d]*Department of Surgery, Cornell University, New York, NY, U.S.A.*

Received 3 March 1998

Abstract

Axial and radial specimens of non-degenerate and degenerate human anulus fibrosus (AF) were tested in confined compression to test the hypothesis that degeneration significantly affects the compressive properties of AF. Due to the highly oriented structure of AF, a secondary objective was to investigate anisotropic behaviors of AF in compression. Uniaxial swelling and stress–relaxation experiments were performed on site-matched samples of anulus from the anterior outer region of L2–3 intervertebral discs. The experimental stress–relaxation behavior was modeled using the finite deformation biphasic theory and a finite-difference approximation scheme. Significant effects of degeneration but not orientation were detected for the reference stress offset, σ_{offset}, and parameters describing the compressive stiffness (i.e. reference aggregate modulus, H_{A0}, and nonlinear stiffening coefficient, β). Average values were 0.13 ± 0.06 and 0.05 ± 0.05 MPa for σ_{offset}, 0.56 ± 0.21 and 1.10 ± 0.53 MPa for H_{A0} and 2.13 ± 1.48 and 0.44 ± 0.61 for β for all normal and degenerate specimens, respectively. No significant effect of degeneration or orientation were detected for either of the parameters describing the strain-dependent permeability (i.e. reference permeability, k_0, and strain-dependent permeability coefficient, M) with average values for all specimens of $0.20 \pm 0.10 \times 10^{-15}$ m^4/N–s and 1.18 ± 1.30 for k_0 and M, respectively. The loss of σ_{offset} was compensated with an elastic stiffening and change in the shape of the equilibrium stress–strain curve with H_{A0} for degenerate tissues almost twice that of normal tissues and β less than one sixth. The increase in reference elastic modulus with degeneration is likely related to an increase in tissue density resulting from the loss of water content. The significant effects of degeneration reported in this study suggested a shift in load carriage from fluid pressurization and swelling pressure to deformation of the solid matrix of the AF. The results also suggest that the highly organized and layered network of the anulus fibrosus, which gives rise to significant anisotropic effects in tension, does not play a major role in contributing to the magnitude of compressive stiffness or the mechanisms of fluid flow of the anulus in the confined compression configuration.

Keywords: Spine; Intervertebral disc; Aging; Material properties; Hydraulic permeability

1. Introduction

The intervertebral disc is a complex structure that transmits and distributes large loads on the spine while providing flexibility. Located on the radial periphery of the intervertebral disc, the anulus fibrosus (AF) is believed to experience a combination of compressive, tensile and shear stresses during weight-bearing and intervertebral joint motions (Galante, 1967; Nachemson, 1960; Shirazi-Adl, 1989). Failure of this highly structured material is a frequent clinical finding believed to contribute to the etiology of disc degeneration and other symptomatic disc disorders (Videman and Battie, 1996). The AF consists of a fibrous collagen matrix embedded within an aqueous gel of proteoglycans, water and other proteins. Organizationally, it forms distinct layers (or lamellae) that attach to the superior and inferior vertebral bodies (Fig. 1). The orientation of the fibers varies

* Corresponding author. Tel.: (802) 656-4246; fax: (802) 656-4247; e-mail: iatidis @salus.med.uvm.edu.

0021-9290/98/$19.00
PII S0021-9290(98)00046-3

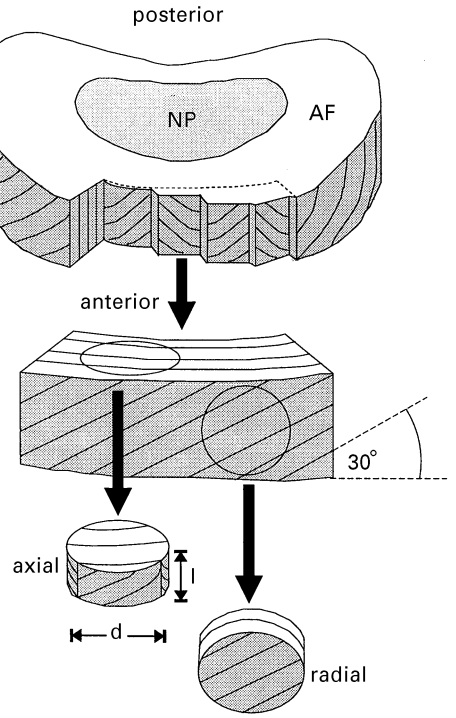

Fig. 1. Diagram of human lumbar intervertebral disc and anulus fibrosus dissection with some layers cut away to display anulus structure. Paired cylindrical specimens were harvested from the anterior outer region of anulus fibrosus from L2–3 discs with axial and radial orientations. Axial and radial correspond to orientations parallel and perpendicular to the vertebral body line of the spine, respectively. Cylindrical samples had average characteristic dimensions $d = 5$ mm and $l = 1.6$ mm. Note that layer thickness and number of fiber bundles per layer are depicted to clarify the multiple layer structure and are not drawn to scale. Layers are roughly 0.1–0.3 mm thick with approximately 40 fiber bundles per layer alternating at angles of roughly $\pm 30^\circ$ (Marchand and Ahmed, 1990).

between successive lamellae, alternating at approximately $\pm 30^\circ$ to the transverse plane of the disc (Galante, 1967; Marchand and Ahmed, 1990). Changes in composition and structure of the AF with degeneration suggest that associated mechanical changes occur. Most strikingly, interstitial pressure in the disc in situ decreased in magnitude with aging and degeneration with values as low as zero for severely degenerated discs (Nachemson, 1960; Panjabi et al., 1988; Urban and McMullin, 1988). The Poisson's ratio, tensile failure stress and strain energy density of the AF also decreased significantly with degeneration with some evidence of sensitivity of the tensile modulus to the grade of degeneration (Acaroglu et al., 1995; Galante, 1967). The effect of degeneration on compressive properties of the AF remains largely uninvestigated.

The highly oriented and layered structure of the AF suggests that its material behaviors may be significantly anisotropic. Indeed, anisotropic effects for the AF were reported for tensile tests of single-layer samples of AF (Galante, 1967; Skaggs et al., 1994) and multiple-layer samples tested at various sample orientations (Acaroglu et al., 1995; Adams and Green, 1993; Ebara et al., 1996; Fujita et al., 1995; Galante, 1967; Marchand and Ahmed, 1989; Wu and Yao, 1976). The material structure also gives rise to anisotropic swelling behaviors for the AF which were reported by Urban and Maroudas (1980), who observed AF dimensions increased more in the radial than axial direction when excised and soaked in saline. In a study of the uniaxial behavior of canine AF samples, differences were observed in the transient behavior and equilibrium modulus between axial and radial specimens when subjected to a change in osmotic environment (i.e. swelling) or step compressive load (Drost et al., 1995). These results suggest that anisotropic viscoelastic behaviors may be significant in the AF, although the role of the AF structure in contributing to these anisotropic behaviors is largely unknown. Finally, radiographic studies on healthy human subjects indicated that the anterior portion of the intervertebral disc may be compressed by more than 25% when in a flexed posture as compared to standing erect (Adams and Hutton, 1982) suggesting that large compressive strains can exist in the AF under physiological loading conditions.

The purpose of this study was to test the hypothesis that degeneration significantly affects the compressive properties of the AF. Furthermore, because of the highly oriented structure of the AF, a secondary objective was to investigate anisotropic behaviors of the AF in compression. In this study, the AF was tested in confined compression under conditions of large deformation and at two orientations. In a previous study, the creep behavior of isolated human AF specimens in compression was well described by a linear biphasic model under small strain conditions (i.e. $\sim -10\%$ strain; Best et al., 1994). In this study, we used a finite deformation formulation of the biphasic theory incorporating strain-dependent permeability effects (Holmes and Mow, 1990; Mow et al., 1980) in order to describe the experimental stress–relaxation behavior of AF at higher strains. The mathematical model and experimental data were used to determine intrinsic material coefficients describing the compressive behavior of the AF solid matrix and the matrix permeability to fluid flow. These material parameters were compared for samples of AF of varying degenerative grade and orientation. Specimen age and water content were also determined and compared with these material parameters to assess the role of age and hydration in influencing the compressive behavior of the AF.

2. Materials and methods

Human lumbar spines (L1–S1) were harvested from cadavers at autopsy at Columbia-Presbyterian Medical Center within 24 h of death as described previously

(Acaroglu et al., 1995). Intervertebral discs from level L2–3 were isolated from the spines and immediately wrapped in clear plastic to minimize dehydration and allow for visual inspection. Discs were morphologically graded using a five class scheme (Acaroglu et al., 1995; Thompson et al., 1990); a wide range in cadaver age (range: 12–83 y; mean = 38.5 y) provided specimens with grades of all 5 classifications. In this scheme, Grade 1 discs have no visible signs of degeneration (discrete lamellae, white in color) and grade V discs have the most frequent and severe signs of degeneration (mucinous material between lamellae, focal disruptions or clefts, brownish color). Blocks of AF were dissected from the anterior and outer region of human lumbar intervertebral discs and stored at -80°C until the day of testing. While still frozen, the blocks of AF were divided into two adjacent pieces, one each for *axial* and *radial* test specimens. *Axial* and *radial* specimens were defined as those aligned parallel and perpendicular to the vertebral body line, respectively (Fig. 1), where the vertebral body line is the 3D curved line that passes through the centroids of the vertebral bodies (Stokes, 1994). Cylindrical test specimens were procured from the blocks of tissue using a microtome (Cryo-Histomat Model B, Hacker Inst., Fairfield, NJ) and corneal trephine (5 mm dia.) as described previously (Iatridis et al., 1997). The weight and thickness of the frozen specimens were immediately measured. Six thickness measurements were taken across the sample to obtain an average thickness (l) and standard deviation of thickness (δ) for each specimen. Specimens were nearly flat as evidenced by average values of $\delta = 0.04 \pm 0.02$ mm. A total of 44 samples (22 axial, 22 radial) of AF were harvested from 22 L2–3 discs (Grade I: $n = 26$; Grade II, $n = 2$; Grade III: $n = 8$; Grade IV: $n = 6$; Grade V: $n = 2$). Average $\pm$ S.D. thickness (l) of all specimens tested was 1.6 ± 0.3 mm.

While still frozen, samples were placed in the cylindrical confining chamber of a load and displacement controlled apparatus (Guilak et al., 1989) with rigid and porous platens of sintered steel on both faces. These platens had a porosity of $\sim 50\%$, a pore size of 50–80 μm and a permeability of $\sim 1 \times 10^{-10}\,\mathrm{m^4\,N^{-1}s^{-1}}$ (as measured in a direct permeation experiment). The upper platen was connected in series to a load cell (uncertainty = $\pm$ 1 gf) and an LVDT (uncertainty = ± 2.5 μm) in order to record force and displacement, respectively. The upper platen was lowered to a height corresponding to the specimen thickness less one standard deviation ($l_0 = l - \delta$) in order to provide for complete contact of the sample with the platen. Saline (0.15 M NaCl) was added to the chamber and the transient axial force increase was monitored until a steady value was reached at ~ 4000 s. Based on this equilibrium value, a reference stress offset (σ_{offset}) was calculated as axial, compressive force at equilibrium divided by the sample cross-sectional area. The values for σ_{offset} were related to the swelling pressure and its non-zero value suggested the samples interdigitated with the filters and swelled to fill the confining chamber. This equilibrated state was taken as the initial state for the subsequent stress–relaxation tests, where σ_{offset} was subtracted from subsequent stress calculations for definition of a zero stress–strain initial state. The samples were subjected to successive stress–relaxation tests consisting of a 'ramp' phase (during which a compressive displacement was applied to the face of the specimen at a constant stretch rate of $0.0001\ \mathrm{s^{-1}}$) followed by a 'relaxation' phase during which the displacement was held constant for 2500 s. The magnitude of applied displacements corresponded to an axial strain of -0.10 for the first stress–relaxation test, followed by increments of -0.05 strain for subsequent tests until a cutoff force of -900 gf (-0.45 MPa; i.e. the limit of the load cell) was attained. All specimens were subjected to a minimum of three tests. The Cauchy stress (σ, i.e. first Piola–Kirchoff stress) was calculated as the axial force normalized by the sample cross-sectional area, and the stretch (λ) was calculated as the ratio of the deformed and initial thickness (l_0). An equilibrium force ($t \to \infty$) was determined by extrapolating the equilibrium stress response from an exponential fit to the last 1500 s of the relaxation data. This value was used in the determination of an equilibrium compressive stress (σ_{equil}) for each increment of strain. Upon completion of mechanical tests, specimens were lyophilized for 48 h at -50°C to determine specimen dry weight and the water content of each sample was calculated as $\%H_2O = (\text{wet–dry weights})/\text{wet weight}$.

A finite deformation biphasic theory for intrinsically incompressible mixtures (Cohen, 1992; Holmes and Mow, 1990; Mow et al., 1980) was used to analyze the material behavior of the AF. This continuum theory assumes that the tissue is a mixture of an intrinsically incompressible and elastic solid phase and an intrinsically incompressible and inviscid fluid phase. In this model, viscoelastic effects are attributed to momentum exchange between the solid and fluid phases due to frictional drag. Following Holmes and Mow (1990) and Cohen (1992), the Cauchy stress tensors for the solid and fluid phases and the momentum exchange were defined as

$$\sigma^{\mathrm{s}} = -\phi^{\mathrm{s}} p\mathbf{I} + \sigma^{\mathrm{e}}, \quad \sigma^{\mathrm{f}} = -\phi^{\mathrm{f}} p\mathbf{I}, \tag{1a,b}$$

$$\pi = \mathbf{K}(\mathbf{v}^{\mathrm{f}} - \mathbf{v}^{\mathrm{s}}) + p\nabla\phi^{\mathrm{s}}. \tag{2}$$

In these relations, p is the apparent fluid pressure, σ^{e} is the extra stress tensor for the solid phase and is the elastic portion of the solid stress, $\mathbf{K}$ is a positive definite diagonal tensor describing diffusive drag arising from the relative velocities between fluid ($\mathbf{v}^{\mathrm{f}}$) and solid ($\mathbf{v}^{\mathrm{s}}$) phases. Solid and fluid volume fractions, ϕ^{s} and ϕ^{f}, respectively, were related to their values at the reference state, ϕ^{s}_0 and ϕ^{f}_0, through a dependence on dilatation (Holmes and Mow,

1990). The gradient of the solid volume fraction in Eq. (2) is not assumed to be negligible in the finite deformation theory, and may be considered as a buoyancy force arising from a density gradient.

An isotropic form for the constitutive relation of a biphasic mixture was used in this study so that fewer parameters were needed to describe material behaviors. The isotropic formulation provided a relationship between principal components of the extra stress σ^e and the scalar invariants of the left Cauchy–Green deformation tensor of the solid phase (Ateshian et al., 1997; Holmes and Mow, 1990). In confined compression, there is only one non-zero component of deformation, the axial stretch (λ) and only one governing term in the diffusive drag tensor. This diffusive drag coefficient (K) was related to the hydraulic permeability (k) of the tissue under conditions of slow-flow by the relation, $K = (\phi^f)^2/k$ (Lai and Mow, 1980). The constitutive relation for the axial component of Cauchy stress and axial stretch reduced to the following,

$$\sigma_z^e = \frac{1}{2}H_{A0}\left(\frac{\lambda^2 - 1}{\lambda^{2\beta+1}}\right)\exp[\beta(\lambda^2 - 1)]. \quad (3)$$

Stretch was related to the axial deformation, $U(Z,t)$, as $\lambda = (1 + \partial U(z,t)/\partial Z)$, where Z is the axial material coordinate and t is time. Two material parameters described the equilibrium, elastic stress response of the solid phase: the zero-strain aggregate modulus, H_{A0}, and the nonlinear stiffening coefficient, β. A strain-dependent form of the hydraulic permeability was given by

$$k = k_0\left(\frac{\phi_0^s\,\phi^f}{(1 - \phi_0^s)\phi^s}\right)\exp\,[M(\lambda^2 - 1)/2]. \quad (4)$$

In this expression, the strain-dependent permeability, k, was characterized by the material coefficients k_0 and M representing the zero-strain permeability and the nondimensional non-linear permeability coefficient, respectively. For the problem of uniaxial confined compression, the governing equations for finite deformation of the tissue reduce to a single, non-linear partial differential equation (Holmes, 1986):

$$\frac{\partial\sigma_z^e}{\partial\lambda}\frac{\partial^2 U}{\partial Z^2} = \frac{\lambda}{k}\frac{\partial U}{\partial t} \quad 0 < Z < h,\ t > 0. \quad (5)$$

Two boundary conditions and one initial condition were required for the stress–relaxation test as follows:

$$U(Z = h, t) = 0, \quad U(Z = 0, t) = \begin{cases} V_0 t, & 0 \leqslant t \leqslant t_0 \\ V_0 t_0, & t > t_0 \end{cases}, \quad (6a,b)$$

$$U(Z, t = 0) = 0, \quad (6c)$$

where h is the deformed tissue thickness, V_0 is the displacement rate and t_0 is the ramp time. The system of partial differential equations defined by Eqs. (3)–(5) and the initial and boundary conditions given in Eqs. (6), were solved numerically using the method of finite differences. The discretization method utilized a central difference scheme in space (mesh size = 40 space intervals over total thickness) and backward difference approximation in time (time step = 20 s) to yield an implicit scheme for the dependent variable U (Ateshian et al., 1997). The resulting non-linear tri-diagonal system of equations was solved at each time step using the Newton–Raphson method.

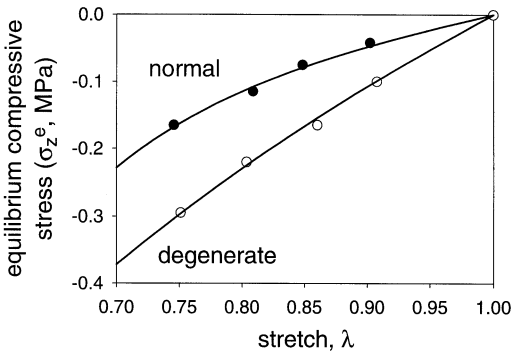

Fig. 2. The equilibrium elastic stress–stretch response of a normal (grade I) and degenerate (grade IV) AF specimens determined from the stress–relaxation experiments. This $\sigma_z^e - \lambda$ behavior was non-linear indicating stiffness increased with compressive strain. This curve was used to determine the material parameters describing the compressive stiffness, i.e. reference aggregate modulus (H_{A0}) and nonlinear stiffening coefficient (β). Excellent agreement was observed between the experimental data and theoretical model. In general, degenerate specimens were stiffer and more linear than normal specimens. Note that the stress is calculated as the first Piola–Kirchoff stress (σ).

The finite deformation biphasic theory used 4 material parameters to describe the experimental behavior of the AF in confined compression: H_{A0}, β, k_0, and M. For all analyses, a 2-step procedure was used to determine these parameters. First, the parameters describing the elastic behavior of the solid matrix, (H_{A0}, β), were determined by non-linear regression of Eq. (3) to the equilibrium stress–stretch data (Fig. 2, regression performed using: FITFUNCTION, RS/1, BBN Software Products, Cambridge, MA). Using the determined values for H_{A0} and β, the parameters describing the hydraulic permeability (k_0 and M) were then determined by non-linear regression of the numerical solution for the axial stress to the experimental stress– relaxation data from the first three experiments (DBCONF, IMSL Inc., Houston, TX) (Ateshian et al., 1997). In this procedure, the finite difference solution was used for each iteration until convergence was reached (convergence criterion: change in residual error $\leqslant 5 \times 10^{-7}$ MPa). From this analysis, best-fit parameters were obtained (Fig. 3a). For all samples, ϕ_0^s was taken as 0.3 based on values for water content for AF of roughly 70% (Antoniou et al., 1996; Best et al., 1994; Urban and McMullin, 1988). In order to test the

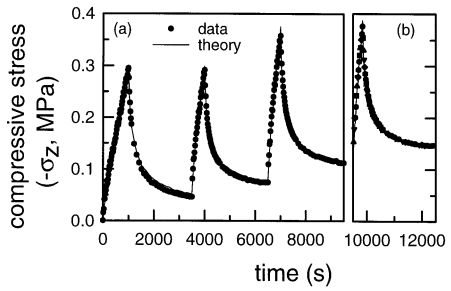

Fig. 3. Transient stress–relaxation behavior for the same normal AF specimen as in Fig. 2. The strain-dependent permeability parameters (k_0, M) describing the rate of fluid flow through the solid matrix were determined though nonlinear regression of the experimental data to a finite difference solution of the governing equations for the first three experiments. (a) The determined material parameters were then used to predict the final stress–relaxation experiment; (b) the model exhibited very close agreement with the experimental data for the curve-fit and for the predicted stress–relaxation experiment.

predictive ability of the biphasic model for describing the non-linear compressive behavior of the AF, the theoretical solution and material parameters determined from the first 3 tests were used to predict the remaining stress–relaxation tests, for those samples in which more than three successive stress–relaxation tests were performed (Fig. 3b).

For statistical purposes, specimens were separated into two degenerative levels (normal: Grades I and II, $n = 28$ vs degenerate: Grades III–V, $n = 16$). Two-way ANOVA was used to test for effects of degeneration and sample orientation (radial vs axial) on the variables σ_{offset}, H_{A0}, β, k_0, and M. Linear correlation analyses of specimen age, degenerative grade, and water content were performed against all material properties. Correlation analyses were performed on degenerative grade to assess similarities of the relationships of age and degenerative grade with material parameters. The results of the correlation analyses (correlation coefficient, r) and all statistical analyses are presented at a significance level of $p < 0.05$. All statistical analyses were performed using SAS statistical software (SAS Institute Inc., Cary, NC).

3. Results

All AF specimens exhibited a monotonic increase in axial force immediately after exposure to 0.15 M NaCl in the confining chamber from which the reference stress offset was calculated. The value of σ_{offset} significantly decreased with degenerative grade but was not affected by orientation (Fig. 4) with mean $\pm$ S.D. values of 0.126 ± 0.056 and 0.050 ± 0.046 MPa for normal and degenerate specimens, respectively. A significant interaction between factors degeneration and orientation was detected for σ_{offset} indicating that the value for σ_{offset} decreased more with degeneration for radial specimens than for axial specimens.

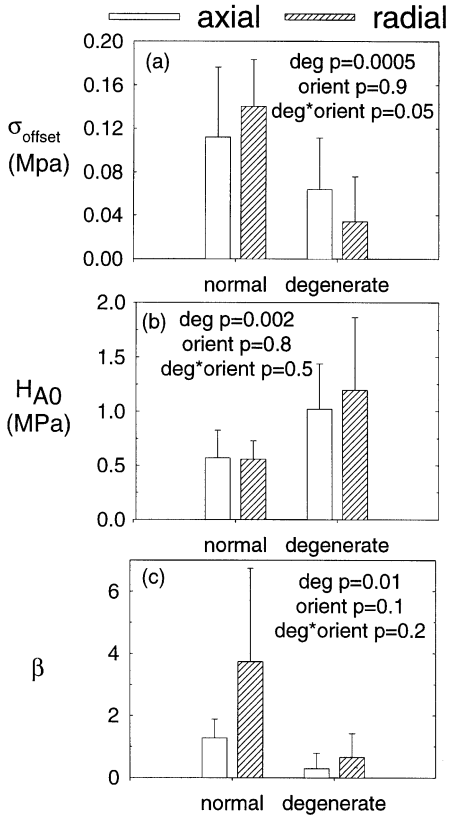

Fig. 4. Compressive material properties governing the reference stress offset and equilibrium elastic stress–stretch response of the AF. Significant effects of degeneration were detected for the (a) reference stress offset, σ_{offset}, (b) reference aggregate modulus, H_{A0}, and (c) non-linear stiffening coefficient, β. No significant effects of orientation were detected. Results suggest a loss of swelling pressure and residual stress with degeneration that is larger in the radial than axial orientations. The AF compensates through an elastic stiffening of the AF, represented by the increase in H_{A0}. Further, alterations in structure and composition of the AF with degeneration are manifested in a loss of non-linearities in the elastic behavior, represented by a decrease in β.

During the ramping phase of the stress–relaxation test, the stress increased rapidly with a generally convex shape (Fig. 3a). As the displacement was held constant, the stress relaxed rapidly to a value which approached equilibrium after 2500 s. The experimental values for the equilibrium elastic stress–stretch were well described by the mathematical relationship for σ_z^e and λ in Eq. (3) (Fig. 2). The finite difference solution of the biphasic model also exhibited very good agreement with the transient stress–relaxation response for the first three tests (Fig. 3a) as well as for additional predicted tests (Fig. 3b).

Significant effects of degeneration were detected for compressive material properties describing the stiffness (Fig. 4b and c), however, no significant effects of degeneration were detected for parameters describing permeability (Fig. 5a and b). No significant effects of orientation

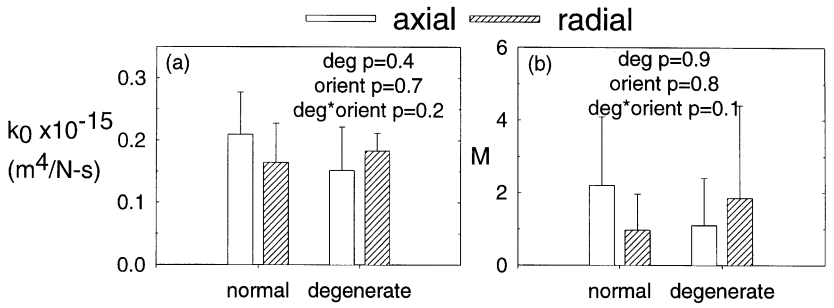

Fig. 5. No significant effects of degeneration or orientation were detected for either the (a) reference permeability, k_0, or the (b) strain-dependent permeability coefficient, M.

were detected for any compressive material properties. Mean $\pm$S.D. values were 0.56 ± 0.21 and 1.10 ± 0.53 MPa for H_{A0}, and 2.13 ± 1.48 and 0.44 ± 0.61 for β for all normal and degenerate specimens, respectively. The 95% confidence intervals for all specimens were 0.57–0.74 MPa and 0.98–1.90 for H_{A0} and β, respectively. No significant effect of degeneration or orientation was detected for either of the parameters describing the strain-dependent permeability with average values for all specimens of $0.21 \pm 0.10 \times 10^{-15}\,m^4\,N^{-1}\,s^{-1}$ (95% confidence interval: $0.18–0.23 \times 10^{-15}\,m^4\,N^{-1}\,s^{-1}$) and 1.18 ± 1.30 (95% confidence interval: 0.83–1.54) for k_0 and M, respectively. All material parameters were statistically different from zero ($p < 0.0001$). The non-zero values for parameters β and M indicated samples exhibited non-linear equilibrium stress–stretch behavior and strain-dependent permeability. The significant decrease in β with degeneration indicated that the stress–stretch relationship for degenerate specimens was more linear than for normal specimens.

Specimen age exhibited significant but weak correlations with material parameters σ_{offset} ($r = -0.40$) and H_{A0} ($r = 0.41$). A low negative relationship was found for age with β ($r = -0.31$), however, this was not statistically significant ($p = 0.09$). Specimen age had a high positive correlation with degenerative grade ($r = 0.85$). In general, degenerative grade had very similar relationships with material parameters σ_{offset} ($r = -0.54$), H_{A0} ($r = 0.46$), and β ($r = -0.36$) as specimen age. Significant effects of degeneration ($p = 0.02$) were detected for water content with average values of $65 \pm 7\%$ and $57 \pm 7\%$ for normal and degenerate specimens, respectively. Significant correlations were detected for water content with age ($r = -0.53$) and degenerative grade ($r = -0.48$), however, water content did not significantly correlate with any material parameters.

4. Discussion

Normal and degenerate AF specimens with axial and radial orientations were tested in confined compression under conditions of large deformation to test the hypotheses that degeneration and specimen orientation significantly affect the compressive properties of the AF. Successive stress–relaxation experiments were performed on AF samples. The experimental stress–relaxation response was modeled using a finite deformation biphasic theory and a finite-difference approximation scheme. Material parameters describing nonlinear behaviors of the solid matrix in compression (H_{A0}, β) and the strain-dependent permeability (k_0, M) were determined from the experimental stress–relaxation response and validated using data from successive stress–relaxation experiments. Specimen age and water content were determined to test for relationships between parameters of the compressive behavior and specimen age and hydration.

There were several limitations of this study which impact upon interpretation of the findings. First, the reference stress offset was measured as a parameter of initial, non-zero stresses in the AF due to osmotic forces. The non-zero value of σ_{offset} indicated that there were residual stresses in our reference configuration and also a compressive offset strain (i.e. residual strain) that was necessary to prevent free swelling. Therefore, the reference state for stress–stretch calculation was chosen to be nearly the physiological post-mortem deformational state. Importantly, average values for σ_{offset} of 0.10 MPa compared well with values for hydrostatic or osmotic pressures of the AF measured using pressure transducers or osmometry techniques (Glover et al., 1991; McNally and Adams, 1992; Nachemson, 1960; Urban and McMullin, 1988). While the choice of reference state for a non-linear formulation will influence values for material parameters, the exact choice of reference state for this study should not have a large impact on the material properties and stress-stretch behavior since results were valid over a large range of strains.

Additional limitations were introduced by the constraints of the testing conditions. Since the filter/platen was 50% porous with pore size 50–80 μm, we assumed that 50% of the tissue surface interdigitates completely (i.e., 50–80 μm) into the pores of the filter. Interdigitation

can influence the stress response and was expected to be very small for the low frequency tissue response of our tests (Buschmann et al., 1995; Mow et al., 1980). Also, in many cases, test samples did not reach an equilibrium stress state in the 2500 s relaxation period and required an exponential extrapolation to obtain estimates of equilibrium stress values. This relatively short relaxation time was used to minimize potential leaching or degradation of matrix macromolecules over the roughly 4 h test period. A previous study using a similar protocol showed no change in σ_{offset} (i.e. in that study σ_{offset} was defined as P_{sw}) or aggregate modulus within the first 20,000 s of testing suggesting that potential leaching or specimen degradation did not influence results (Best et al., 1994).

In this study, specimens were obtained from the anterior outer region of the anulus fibrosus only because this region is not commonly associated with anulus failure. While the effects of axial and radial orientations were evaluated, complete characterization of the anisotropic nature of the AF in confined compression would require additional tests on specimens with circumferential orientations (i.e. aligned with the layers of the AF) and in various locations about the intervertebral disc. Heterogeneity of the compressive properties of lumbar AF was the subject of a previous investigation (Best et al., 1994) and thus was not studied here. The simplifying use of isotropic constitutive relations may interfere somewhat with our ability to detect anisotropies, however, a more complicated anisotropic constitutive law was not investigated because no evidence of anisotropic behaviors was detected. Fissures present in the degenerate AF were avoided during specimen harvest and may have a strong influence on material behavior of the AF in situ. Based on available specimens, the effect size desired to detect ($\delta/2\sigma = 0.4$, considered a large effect for ANOVA), and with $\alpha = 0.05$, a power analysis resulted in 90% power for the repeated measures factor orientation, and 70% for the factor degeneration, and 70% for the interaction. For material parameters where a significant difference was not detected, we may not conclude that the means are the same since small effects may be present. We may, however, conclude with a high probability that we have properly not rejected the null hypothesis that the difference between means is less than our stated effect size.

Significant effects of degeneration were detected for σ_{offset} and the material parameters describing the compressive stiffness. The decrease in σ_{offset} with degeneration was likely related to the commonly reported loss of proteoglycan content of the AF with age and degenerative grade (Antoniou et al., 1996; Urban and McMullin, 1988). Our finding that σ_{offset} was not sensitive to orientation confirms previous findings (McNally and Adams, 1992; Nachemson, 1960) that in situ swelling pressure measurements are equivalent in both vertical and horizontal directions in the non-degenerate disc. The significant interaction in the value of σ_{offset} between the factors orientation and degeneration are similar to differences in 'swelling pressure' with orientation reported for severely degenerate discs (McNally and Adams, 1992; Nachemson, 1960). In normal tissues, fluid pressurization and swelling pressure is expected to shield the solid matrix from large matrix strains. The loss of radially directed σ_{offset} with degeneration suggested that more of the loads in the degenerate AF were carried via non-hydrostatic (and non-uniform) mechanisms. The loss of σ_{offset} was compensated with an elastic stiffening and change in the shape of the equilibrium stress–stretch curve with H_{A0} for degenerate tissues almost twice that of normal tissues and β less than one sixth. The increase in reference elastic modulus with degeneration is likely related to an increase in tissue density resulting from the loss of water content. The reduction in non-linear behavior ($\beta \downarrow$) with degeneration, however, suggested a diminished compaction effect of the degenerate tissues at large deformations which could be related to structural changes in the matrix. Taken together, these two effects (swelling and elastic) suggest a shift in load carriage from

Table 1
Comparison of finite deformation biphasic material properties for anulus fibrosus and articular cartilage

	Human AF[a] (normal)	Human AF[a] (degenerate)	Human AF, small strain[b]	Canine AF, small strain[c]	Bovine articular cartilage[d]
σ_{offset} (MPa)	0.13 ± 0.06	0.05 ± 0.05	0.11 ± 0.07	—	—
H_{A0} (MPa)	0.56 ± 0.21	1.10 ± 0.53	0.44 ± 0.21	1.01 ± 0.31 (ax) 0.66 ± 30 (rad)	0.40 ± 0.14
β	2.7 ± 2.6	0.44 ± 0.61	—	—	0.35 ± 0.29
$k_0 (\times 10^{-15}\,m^4\,N^{-1}s^{-1})$	0.18 ± 0.07	0.16 ± 0.06	0.25 ± 0.11	0.32 ± 0.15 (ax) 0.18 ± 0.05 (rad)	2.7 ± 1.5
M	1.5 ± 1.6	1.4 ± 1.9	—	—	2.2 ± 1.0

[a] Material parameters are average $\pm$ S.D. values of all normal or degenerate human lumbar AF specimens tested in this study pooled for orientation.
[b] From Best et al. (1994), values for linear biphasic aggregate modulus and permeability of radial specimens from anterior outer region.
[c] From Drost et al. (1995), values for linear biphasic aggregate modulus of axial and radial specimens.
[d] From Ateshian et al. (1997).

fluid pressurization and swelling pressure to deformation of the solid matrix of the AF. The decrease in water content of AF with degeneration would suggest a decrease in permeability based on previous studies documenting a positive correlation between these parameters (Setton et al., 1994). However, the commonly reported loss of proteoglycans with degeneration would also suggest an increase in the permeability of the AF. These two competing effects may explain why significant differences were not found for either of the permeability coefficients with degeneration or water content. Finally, aging and degenerative grade had similar effects on material properties based on similarities of the correlation coefficients.

The results of this study present no evidence of material anisotropy in compression and suggest that fundamental mechanisms for fluid flow through the tissue and compaction of the AF matrix were not *strongly* influenced by the highly oriented and layered fibrous network. While our limited test design prevents a definite conclusion regarding material isotropy, it seems clear that the AF does not exhibit marked differences in compressive properties between axial and radial orientations as it does in tension where the tensile modulus ranges from 0.5 to 140 MPa depending on specimen orientation (Acaroglu et al., 1995; Ebara et al., 1996; Galante, 1967; Marchand and Ahmed, 1989; Wu and Yao, 1976). In contrast, Drost and co-workers (1995) reported differences with orientation in the value of H_A; the difference between these studies could be related to species and experimental conditions (Table 1). Significant anisotropic effects for the AF are expected in other test configurations such as unconfined compression or shear where tensile strains are also generated. The confined compression configuration is an idealized experimental configuration which represents a limiting case of the loading on the AF in vivo. Finite element models incorporating appropriate values for the material parameters of the AF in tension, compression and shear may be useful in predicting the biomechanical roles of AF anisotropy in different loading modes for the disc. The lack of strongly radial and axial effects in compression may be useful, however, when making simplifying assumptions regarding material behavior in finite element models.

Non-linear effects were observed for the material behavior of the AF in both measures of the elastic stress–stretch relationship of the solid matrix and in the hydraulic permeability of the tissue. Non-zero values of β for the AF indicated that non-linearities in the elastic behavior of the solid matrix were present at equilibrium with values similar to that for bovine articular cartilage (Table 1). The reference aggregate modulus was similar to the average values determined previously for the AF using the linear biphasic theory (Table 1). Non-zero values for M in this study give evidence of a significant strain-dependent permeability effect. The reference permeability determined in this study was similar to but somewhat lower than values previously reported for AF and an order of magnitude lower than for cartilage (Table 1). The similarity of material parameters determined using the linear and non-linear theoretical models suggested that the material behavior of the AF may be well-described by a linear model for conditions of small strain (roughly 10%). However, the non-zero values for M and β determined for the AF demonstrate that non-linear effects are significant under large deformation conditions. Model predictions indicate the presence of large surface strains in our test configuration even under relatively slow loading conditions (i.e. $\lambda \sim 0.70$ at the end of the ramp phase from $\lambda = 1.0$ to 0.90 for stretch rate $= -0.0001\ s^{-1}$) indicating that strain rate, boundary conditions, and strain magnitude are all important in determining when the linear and non-linear models should be used. Finally, the large confidence interval for β suggests that this exponential coefficient may be highly sensitive to variations in experimental data for this pool of human specimens.

The experimental stress–relaxation behavior was well described by the finite deformation biphasic model with very little difference between experimental data and model curve-fits and predictions. According to Ateshian et al. (1997), the value of k is relatively insensitive to rather large variations in M, suggesting that determination of permeability parameters through this indirect method may not be that precise. In this study, a constant value of $\phi_0^s = 0.30$ was used for all specimens regardless of degenerative grade. This value has a negligible effect on the ability of the model to describe the stress–relaxation response of the tissue but may influence permeability parameters. Based on a parametric study, altering the value of ϕ_0^s from 0.3 to 0.45 would have a small effect on the value of material parameter k_0 (4% decrease) but more strongly influence the value of M (55% decrease). This result could suggest a decrease in the strain-dependent permeability effect of the degenerate tissue. Direct permeation experiments provide more accurate measurements of permeability parameters for this tissue (Gu et al., 1998).

The intervertebral disc is the largest avascular tissue in the body, depending largely on diffusion and convection for transport of nutrients (O'Hara et al., 1990). The mechanisms for interstitial fluid flow were not found to differ with orientation, as inferred from the values of the strain-dependent permeability parameters, k_0 and M. This finding is physiologically very important since convection can significantly enhance movement of large solutes, such as growth factors, cytokines, and enzymes through the matrix of cartilaginous tissues (O'Hara et al., 1990). Our results suggest that boundary condition effects and not differences in hydraulic permeability with orientation dominate convective transport of solutes in the AF.

In conclusion, significant effects of degeneration on the compressive material properties suggested a shift in load carriage from fluid pressurization and swelling pressure to deformation of the solid matrix of the AF. In normal tissues, fluid pressurization and swelling pressure will shield the solid matrix from deformations. In degenerate tissues there was a loss of swelling pressure, increased matrix deformations, and an associated 'remodeling' of the AF compressive properties. Results also suggested that the highly structured anulus fibrosus, which gives rise to large anisotropic effects in tension, did not play a major role in contributing to the magnitude of compressive stiffness of the anulus in the confined compression configuration. Furthermore, the mechanisms for interstitial fluid flow were not found to differ with orientation, suggesting that, with similar boundary conditions, convective transport of solutes will occur at similar rates from the periphery of the AF as from the end-plate route.

Acknowledgements

This work was supported by funds from the Orthopaedic Research and Education Foundation (CDA, MW), National Science Foundation (BES95-10401, LAS), National Institutes of Health (5-R01-AR-41913) and National Institutes of Health Training Grant (T35AR-07568). The authors gratefully acknowledge the assistance of Gerard Ateshian, Leena Krishnan, and Sheryl Handler on many aspects of this project.

References

Acaroglu, E.R., Iatridis, J.C., Setton, L.A., Foster, R.J., Mow, V.C., Weidenbaum, M., 1995. Degeneration and aging affect the tensile behavior of human lumbar anulus fibrosus. Spine 20, 2690–2701.

Adams, M.A., Hutton, W.C., 1982. Prolapsed intervertebral disc: A hyperflexion injury. Spine 7, 184–191.

Adams, M.A., Green, T.P., 1993. Tensile properties of the anulus fibrosus. I. The contribution of fibre-matrix interactions to tensile stiffness and strength. European Spine Journal 2, 203–208.

Antoniou, J., Steffen, T., Nelson, F., Winterbottom, N., Hollander, A.P., Poole, R.A., Aebi, M., Alini, M., 1996. The human lumbar intervertebral disc: Evidence for changes in the biosynthesis and denaturation of the extracellular matrix with growth, maturation, ageing, and degeneration. Journal of Clinical Investment 98, 996–1003.

Ateshian, G.A., Warden, W.H., Grelsamer, R.P., Mow, V.C., 1997. Biphasic finite deformation material properties of bovine articular cartilage from confined compression experiments. Journal of Biomechanics 30, 1157–1164.

Best, B.A., Guilak, F., Setton, L.A., Zhu, W., Saed-Nejad, F., Ratcliffe, A., Weidenbaum, M., Mow, V.C., 1994. Compressive mechanical properties of the human anulus fibrosus and their relationship to biochemical composition. Spine 19, 212–221.

Buschmann, M.D., Jurvelin, J.S., Hunziker, E.B., 1995. Comparison of sinusoidal and stress relaxation measurements of cartilage in confined compression: The biphasic poroelastic model and the role of the porous compressing platen. Trans. 41st Orthopoedic Research Society 20, 521.

Cohen, B., 1992. Anisotropic hydrated soft tissues in finite deformation and the biomechanics of the growth plate. Ph. D. Thesis, Columbia University, New York, NY.

Drost, M.R., Willems, P., Snijders, H., Huyghe, J.M., Janssen, J.D., Huson, A., 1995. Confined compression of canine annulus fibrosus under chemical and mechanical loading. Journal of Biomechanical Enginering 117, 390–396.

Ebara, S., Iatridis, J.C., Setton, L.A., Foster, R.J., Weidenbaum, M., Mow, V.C., 1996. Tensile properties of non-degenerate human lumbar anulus fibrosus. Spine 21, 452–461.

Fujita, Y., Lotz, J.C., Soejima, O., 1995. Site specific radial tensile properties of the lumbar anulus fibrosus. Transactions of the 41st Annual Meeting of the Orthopaedic Research Society 20, 673.

Galante, J.O., 1967. Tensile properties of the human lumbar anulus fibrosus. Acta Orthop. Scand. Suppl 100, 4–91.

Glover, M.G., Hargens, A.R., Mahmood, M.M., Gott, S., Brown, M.D., Garfin, S.R., 1991. A new technique for the in vitro measurement of nucleus pulposus swelling pressure. Journal of Orthopaedic Research 9, 61–67.

Gu, W.Y., Mao, X.G., Rawlins, B.A., Foster, R.J., Weidenbaum, M., Mow, V.C., 1998. Hydraulic permeability of human lumbar anulus fibrosus depends on direction and degeneration. Transactions of the 44th Annual Meeting of the Orthopaedic Research Society 23, 299.

Guilak, F., Best, B.A., Ratcliffe, A., Mow, V.C., 1989. Instrumentation for load and displacement controlled studies on soft connective tissues. ASME Biomechanics Symposium AMD 98, 113–116.

Holmes, M.H., 1986. Finite deformation of soft tissue: Analysis of a mixture model in uni-axial compression. Journal of Biomechanical Engineering 108, 372–381.

Holmes, M.H., Mow, V.C., 1990. The nonlinear characteristics of soft gels and hydrated connective tissues in ultrafiltration. Journal of Biomechanics 23, 1145–1156.

Iatridis, J.C., Setton, L.A., Weidenbaum, M., Mow, V.C., 1997. The viscoelastic behavior of the non-degenerate nucleus pulposus in shear. Journal of Biomechanics 30, 1005–1013.

Lai, W.M., Mow, V.C., 1980. Drag-induced compression of articular cartilage during a permeation experiment. Biorheology 17, 111–123.

Marchand, F., Ahmed, A.M., 1989. Mechanical properties and failure mechanisms of the lumbar disc anulus. Trans. Orthop. Res. Soc. 14, 355.

Marchand, F., Ahmed, A.M., 1990. Investigation of the laminate structure of lumbar disc annulus fibrosus. Spine 15, 402–410.

McNally, D.S., Adams, M.A., 1992. Internal intervertebral disc mechanics as revealed by stress profilometry. Spine 17, 66–73.

Mow, V.C., Kuei, S.C., Lai, W.M., Armstrong, C.G., 1980. Biphasic creep and stress relaxation of articular cartilage in compression: Theory and experiments. Journal of Biomechanical Engineering 102, 73–84.

Nachemson, A., 1960. Lumbar intradiscal pressure. Acta Orthopaedic Scandinavia Supplement 43, 1–104.

O'Hara, B.P., Urban, J.P.G., Maroudas, A., 1990. Influence of cyclic loading on the nutrition of articular cartilage. Annals of Rheumatic Disease 49, 536–539.

Panjabi, M., Brown, M., Lindahl S., Irstam, L., Hermens, M., 1988. Intrinsic disc pressure as a measure of integrity of the lumbar spine. Spine 13, 913–917.

Setton, L.A., Mow, V.C., Muller, F.J., Pita, J.C., Howell, D.S., 1994. Mechanical properties of canine articular cartilage are significantly altered following transection of the anterior cruciate ligament. Journal of Orthopaedic Research, 12, 451–463.

Shirazi-Adl, A., 1989. On the fibre composite material models of disc annulus: comparison of predicted stresses. Journal of Biomechanics 22, 357–365.

Skaggs, D.L., Weidenbaum, M., Iatridis, J.C., Ratcliffe, A., Mow, V.C., 1994. Regional variation in tensile properties and biochemical composition of the human lumbar anulus fibrosus. Spine 19, 1310–1319.

Stokes, I.A.F., 1994. Three dimensional terminology of spinal deformity. Spine 19, 236–248.

Thompson, J.P., Pearce, R.H., Schechter, M.T., Adams, M.E., Tsang, I.K.Y., Bishop, P.B., 1990. Preliminary evaluation of a scheme for grading the gross morphology of the human intervertebral disc. Spine 15, 411–415.

Urban, J.P.G., Maroudas, A., 1980. The chemistry of the intervertebral disc in relation to its physiological function and requirements. Clinical Rheumatic Disease 6, 51–76.

Urban, J.P.G., McMullin, J.F., 1988. Swelling pressure of the lumbar intervertebral discs: Influence of age, spinal level, composition, and degeneration. Spine 13, 179–187.

Videman, T., Battie, M.C., 1996. A critical review of the epidemiology of idiopathic low back pain. In: Weinstein, J.N., Gordon, S.L., (Eds.), Low back pain: A scientific and clinical overview AAOS, Rosemont, IL, pp. 317–332.

Wu, H.C., Yao, R.F., 1976. Mechanical behavior of the human anulus fibrosus. Journal of Biomechanics 9, 1–7.